

Structure and bonding in liquid tellurium

C. Bichara

Centre de Thermodynamique et de Microcalorimétrie, CNRS 26, rue du 141^{ème} R.I.A., F13331 Marseille, France

J.-Y. Raty and J.-P. Gaspard

Condensed Matter Physics Laboratory, University of Liège, B4000 Sart Tilman, Belgium

(Received 24 July 1995)

The atomic structure and bonding mechanism in liquid tellurium have been investigated by a tight-binding Monte Carlo simulation. On melting, the chain structure of the crystal is preserved in spite of some significant changes in the local atomic environment. A third covalent bond appears with a bond length (widely distributed around 3.15 Å) intermediate between those characteristic of the crystal. A short-long alternation of the bonds takes place within the chains, in agreement with the most recent extended x-ray-absorption fine structure measurements. In addition, the bond angle within the chains is reduced. Our calculations clearly prove that these effects are due to the electronic interaction between the lone pair orbitals. The subsequent broadening of the lone pair band is responsible for the semiconductor to metal transition that takes place upon melting.

INTRODUCTION

The atomic structure as well as the chemical bonding processes in liquid tellurium have been long-standing questions from both theoretical and experimental points of view. Crystalline tellurium is a twofold-coordinated semiconductor that becomes a poor metal upon melting.¹ The early measurements made by Tourand and Breuil² eventually turned out to be incorrect due to the smaller scattering vector range available experimentally at that time. Since then, a large number of x-ray,³ neutron diffraction,^{4–11} or extended x-ray-absorption fine structure¹² (EXAFS) data have become available. The interpretation of the pair correlation function usually starts from either the chain structure of the crystal or from the threefold-coordinated random network first proposed by Cabane and Friedel.¹³ The generally accepted value of the coordination number is about 2.5 at the melting point ($T_m=450$ °C) and reaches 3 at higher temperatures. These values are not compatible with a pure chain structure. Indeed, a molecular-dynamics simulation of the structure of the liquid based on effective interatomic forces derived from pseudopotential theory¹⁴ describes the structure in terms of “entangled broken chains.” Among others, Menelle *et al.*⁸ suggested a splitting of the first coordination shell into two different kinds of atoms: the two covalently bound atoms corresponding to the crystal structure and a third atom at a slightly larger distance. In such a picture of the liquid, the 2.5–3 first neighbors are not equivalent and the objection against the Cabane-Friedel model raised by Cutler¹⁵ concerning the electrical properties of the melt no longer holds. Enderby and Barnes¹⁶ thus conclude that there is a substantial penetration of the first coordination shell by nonbonded tellurium atoms. It is now suggested that the two neighbors of an atom belonging to the same chain might be inequivalent and that short and long first neighbor distances are observed in the undercooled liquid¹⁷ and, more recently, in the liquid near the melting point.¹⁸ Assuming that there are twofold- and threefold-coordinated atoms in the liquid, the question of the homogeneity of the melt has been raised.

Takeda *et al.*⁵ explain the temperature dependence of the structure factor by assuming a chemical equilibrium between twofold- and threefold-coordinated tellurium atoms. Along the same line, Tsuchiya and Seymour¹⁹ were able to describe the unusual variations of the adiabatic compressibility, thermal expansion coefficient, and constant-pressure specific heat with temperature by using a model based on a description of the melt with two phases, a metallic one and nonmetallic one.

Apart from the work of Hafner,¹⁴ which relies on a pseudopotential approximation that is questionable for covalent materials that scatter strongly the valence electrons, no successful computer simulation of the liquid has been reported. In particular, contrary to selenium,²⁰ Car-Parrinello-type *ab initio* molecular dynamics has not been applied to the study of liquid tellurium. This can be related to the difficulties encountered within the local density approximation (LDA) to stabilize the crystal structure of selenium or tellurium.²¹

The purpose of this paper is to present the results of recent tight-binding Monte Carlo computer simulations. It is organized as follows. The model is briefly presented in the first paragraph, as well as the computer simulation technique. The choice of the parameters of the model is discussed. The results of the simulations are shown to be in good agreement with the available experimental data. On this basis, the changes in the atomic and electronic structures upon melting are analyzed. Finally, the validity of the various interpretations concerning the atomic and electronic structure of the liquid is discussed, and the crucial role of the interchain interactions is emphasized.

MODEL AND SIMULATION

The model is basically the same as used in previous studies of liquid As, Sb,²² and Se.²³ The total energy is the sum of an attractive electronic term, calculated in a tight-binding approximation, and an empirical repulsive term. The attractive energy (E_a) is due to the broadening of the electronic

TABLE I. Values of parameters used.

$\beta_{ss\sigma}^0$	$\beta_{sp\sigma}^0$	$\beta_{pp\sigma}^0$	$\beta_{pp\pi}^0$	V_0	p
-0.825 eV	1.696 eV	2.231 eV	-0.826 eV	2.801 eV	6.75

levels into a band of partially filled states. It writes

$$E_a = \int_{-\infty}^{E_f} E n(E) dE, \quad (1)$$

where $n(E)$ is the electronic density of states and E_f the Fermi level. The electronic density of states is approximated at the fourth-moment level. The p electron resonance plays the major role in the stabilization of the structure. As the p band is two-thirds filled, the Peierls distortion mechanism leads to a structure with two short and four long bonds around each atom, forming chains in the stable (trigonal) crystalline phase at normal pressures. The s electrons are also included. They tend to increase the bond angle from 90° , a value expected for a pure $pp\sigma$ interaction in a simple tight-binding scheme to 101° . In this model, the only interactions between the chains are resonant electronic interactions leading to a covalent bond. The other contributions to the total energy, among which the long-range dispersion forces are not explicitly included. In order to account for the missing dispersion forces, a constant pressure is applied, the value of which is of the order of magnitude of the internal pressure due to van der Waals forces. In a pure tight-binding model at zero pressure, the Peierls distortion mechanism leads to a complete separation of the chains.²⁴ The tight-binding resonance integrals are assumed to vary with the distance following

$$\beta_\lambda = \beta_\lambda^0 \left(\frac{r}{r_0} \right)^{-q_\lambda} F \left(\frac{r}{r_0} \right), \quad (2)$$

where the symbol λ denotes the $ss\sigma$, $sp\sigma$, $pp\sigma$, and $pp\pi$ interactions and $r_0=2.86 \text{ \AA}$ is a distance unit. For all interactions, $q_\lambda=2$. The damping term

$$F \left(\frac{r}{r_0} \right) = \left[1 + \exp \left(\frac{r/r_0 - \alpha}{\delta} \right) \right]^{-1} \quad (3)$$

is a Fermi function, in a similar manner as that used by Goodwin *et al.*²⁵ in the case of silicon, but with a different analytic dependence. This term is necessary to treat the stronger first-neighbor interactions (around 2.86 \AA) and the weaker long-bond interactions (around 3.45 \AA) within the same formalism. After many trials, it turned out that the dependence of the resonance integrals with distance cannot be reasonably approximated by a simple power or exponential law in the broad distance range considered. The values $\alpha r_0=3.16 \text{ \AA}$ and $\delta r_0=0.226 \text{ \AA}$ are fixed *a priori*, as well as the cutoff distance setting the range of the interactions for the moments calculation, which is fixed at 4.20 \AA .

As usual in a semiempirical tight-binding approach,²⁶ a repulsive term (E_r) is added to prevent the atoms from collapsing. It is given by

$$E_r = \frac{1}{2} \sum_{i \neq j} V_0 \left(\frac{r}{r_0} \right)^{-p} F \left(\frac{r}{r_0} \right). \quad (4)$$

The atomic energy levels ($\epsilon_s=-17.11 \text{ eV}$ and $\epsilon_p=-8.59 \text{ eV}$) are taken from Harrison.²⁷ The remaining adjustable parameters β_λ^0 , V_0 , and p are fitted so as to (i) obtain the correct cohesive energy ($E_c=-2.23 \text{ eV/atom}$), (ii) stabilize the trigonal phase at the correct density (0.0296 \AA^{-3}), and (iii) stabilize the monoclinic high-pressure phase²⁸ and the β -Po phase²⁹ in the correct pressure ranges. The values of the parameters used are listed in Table I. With these parameters the transition pressures at 0 K are 4.8 GPa for the trigonal-to-monoclinic transition (5 GPa experimentally) and 6.7 GPa for the monoclinic to β -Po phase (9 GPa experimentally).

In order to estimate a melting temperature and to follow the variation of the density of the melt with the temperature, a constant-pressure Monte Carlo algorithm has been used. This is classically done³⁰ by alternating a series of atomic displacement steps and volume changes during the course of the simulation. A minimum of 4000 displacement steps and 400 volume change steps per atom have been done for each run, ensuring a good convergence of the density, enthalpy, and structural properties of the liquid. Two series of calculations have been performed with 144 and 1152 atoms, respectively, starting from the trigonal crystal and gradually raising the temperature up to $890 \text{ }^\circ\text{C}$. Such large systems can only be dealt with in the approximate scheme presented here. The external pressure has been chosen so as to obtain the experimental density³¹ just above the melting point ($d=0.0272 \text{ \AA}^{-3}$ at $T=475 \text{ }^\circ\text{C}$) and is fixed at this value throughout the computations.

RESULTS

Apart from giving a correct order of magnitude for the transition pressures between the various high-pressure crystalline phases, the model can be validated by comparing the calculated values of some quantities of interest to the experimental ones.

The melting temperature of the simulated samples lies between 310 and $365 \text{ }^\circ\text{C}$, somewhat below the experimental melting temperature ($450 \text{ }^\circ\text{C}$). No attempt has been made to obtain more accurate values. The density, not presented here, is in agreement with the experimental one, with fluctuations that are rather large because of the small size of the system.

Figures 1 and 2 show the structure factors and the pair correlation functions obtained for 1152 atoms at two different temperatures (480 and $770 \text{ }^\circ\text{C}$). They are compared to the experimental data obtained by Menelle *et al.*⁸ Good agreement is obtained between the experimental and calculated values of the structure factor, except for the amplitude at large scattering vectors (q) where the neutron scattering structure factor $S(q)$ is more damped than the simulated one. Two reasons can be invoked to explain this behavior. First, the large- q behavior of the structure factor is related to the shape of the first peak of the pair correlation function, which is sharper than the experimental one, indicating that the first-neighbor bonds are too stiff. This has to be related to the fact

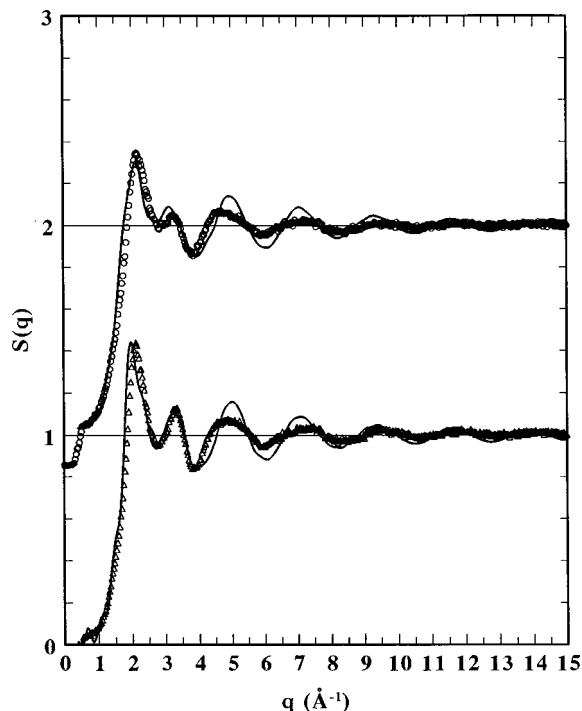


FIG. 1. Lower part: structure factor $S(q)$ calculated at $T=480$ °C for 1152 atoms (solid line), compared to the experimental one (Ref. 8) at 475 °C (symbols). Upper part: structure factor $S(q)$ calculated at $T=770$ °C for 1152 atoms (solid line), compared to the experimental one (Ref. 8) at 750 °C (symbols).

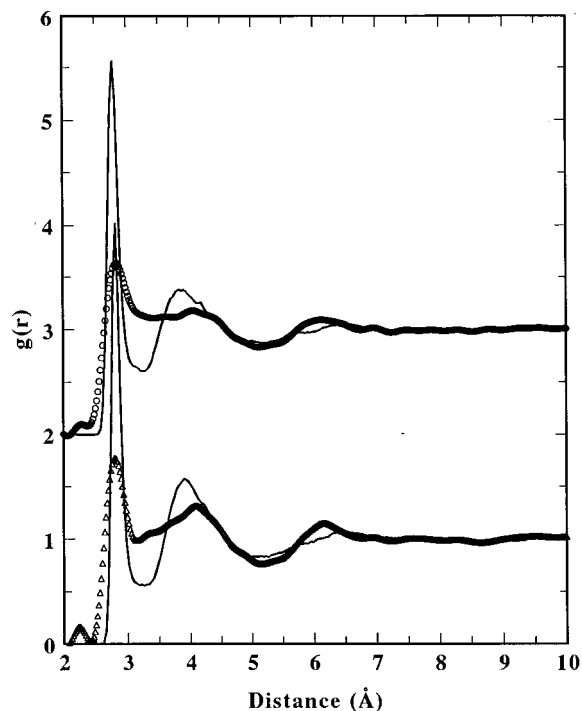


FIG. 2. Lower part: pair correlation function $g(r)$ calculated at $T=480$ °C for 1152 atoms (solid line), compared to the experimental one (Ref. 8) at 475 °C (symbols). Upper part: pair correlation function $g(r)$ calculated at $T=770$ °C for 1152 atoms (solid line), compared to the experimental one (Ref. 8) at 750 °C (symbols).

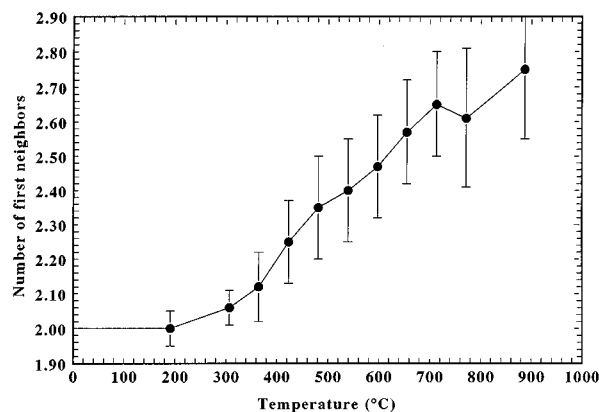


FIG. 3. Number of first neighbors vs temperature (simulation with 144 atoms). The error bars indicate the variations of the number of first neighbors due to the uncertainties on the location of the first minimum of the radial distribution function.

that the bulk modulus of the crystal is overestimated in our calculations. Second, the computed structure factor is calculated by taking the Fourier transform of the pair correlation function, which is directly deduced from the atomic positions, whereas the experimental one is damped by the transfer function of the experimental device. The first peak of $g(r)$ is sharper than the experimental one, leading to a less ambiguous definition of the number of first neighbors (N_1). The variation of N_1 with temperature is plotted in Fig. 3. The error bars indicate the uncertainties in N_1 due to the statistical noise on $g(r)$ that hampers a precise the location of the first minimum of the radial distribution function, the upper integration bound to calculate N_1 . The values of N_1 (between 2.1 and 2.8 in the liquid) are a little below those cited in the literature,⁸ but it has to be stressed that the experimental number of first neighbors is difficult to determine and what is most important is its evolution with temperature. Furthermore, as will be discussed below, such a crude definition of the number of first neighbors is not very meaningful. Considering the overall agreement of the simulation results with the experiments, it is possible to discuss the atomic and electronic structure.

ATOMIC STRUCTURE

The first striking feature is the change of the bond angle distribution (BAD) upon melting, as can be seen in Fig. 4 which presents the BAD calculated on the system of 1152 atoms at three different temperatures: $T=310$ °C (solid), $T=480$ °C, and $T=770$ °C (both liquid). The BAD presents a maximum around 103° in the solid that is shifted towards 95° upon melting. This behavior can also be observed in the experimental pair correlation function: The peak around 4.45 Å, which corresponds to the second-neighbor distance within the crystal chains, has been shifted towards lower distances in the liquid, indicating that the bond angle has been reduced. The dihedral angle distribution (not presented here) is nearly flat in the liquid, exhibiting no peculiarities at the above-mentioned temperatures.

With a cutoff distance taken at the first minimum of the radial distribution function, twofold- (Te^{II}) and threefold- (Te^{III}) coordinated sites can be defined and the atomic struc-

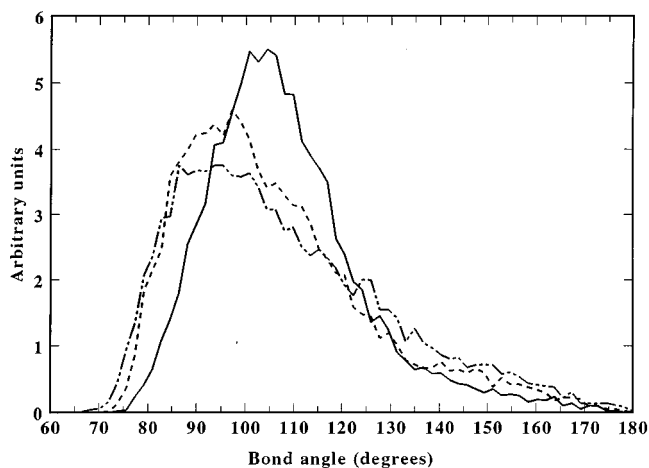


FIG. 4. Bond angle distribution at three different temperatures: solid line, $T=310$ °C (solid); dashed line, $T=480$ °C (liquid); dash-dotted line, $T=770$ °C (liquid).

ture can be described as “entangled broken chains.” The average chain length, calculated on the system of 1152 atoms, is 5.1 bonds at 480 °C and 3.3 bonds at 770 °C. A chain is defined here as a set of connected Te^{II} atoms. In most of the cases, the chains end by a Te^{III} atom connecting three chains. The spatial correlation between Te^{II} and Te^{III} is not random. The Warren-Cowley order parameter (α_1), generalized for the liquids by Wagner and Ruppertsberg³² is defined by

$$\alpha_1 = \left(1 - \frac{Z_{23}}{c_3(c_3Z_2 + c_2Z_3)} \right) / \left(1 - \frac{Z_2}{c_3(c_3Z_2 + c_2Z_3)} \right), \quad (5)$$

where c_2 and c_3 are the concentrations of Te^{II} and Te^{III} , $Z_2=2$ and $Z_3=3$ their coordination numbers, and Z_{23} the average number of Te^{III} surrounding a Te^{II} atom. α_1 varies between 0.59 at 480 °C and 0.41 at 770 °C with increasing temperature, positive values that indicate a tendency to phase separation between Te^{II} and Te^{III} in the melt.

The limits of such a crude definition of bonding in the liquid state clearly appear in a more detailed analysis of the structure. Valuable insight into the atomic structure is gained by separating the contributions of the different first neighbors to the pair correlation function. As can be seen in Fig. 5, the coordination shell of the solid (two first neighbors at 2.86 Å plus four neighbors at 3.45 Å) is modified upon melting. In particular, a third-neighbor contribution appears at intermediate distances (around 3.10 Å) in agreement with the observation made by different authors^{8,16,18}. The bonding of this third atom is clearly covalent. The coordination number can then be defined as $2+\epsilon$, with ϵ varying between 0 and 1 with increasing temperature. Adopting this view, the chain structure of the crystal is preserved upon melting, and one of the interchain bond lengths is reduced. The effect of this strengthening of one of the interchain bonds on the electronic structure is discussed in the next section. A second feature is the splitting of the first peak of $g(r)$, which already appears in the crystalline state at nonzero temperature, but is more pronounced in the liquid and remains in the undercooled liquid at low temperature. Such a splitting has been recently

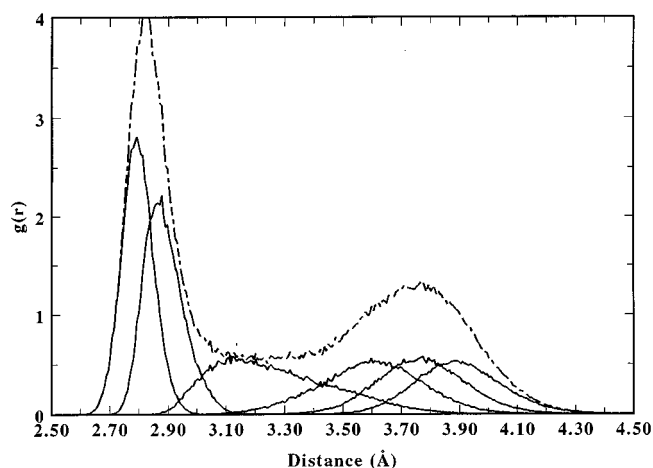


FIG. 5. Solid lines. detailed contributions to the pair correlation function at $T=480$ °C. Dashed line total pair correlation function.

observed by EXAFS measurements^{12,18} and the values of the distances (2.80 and 2.90 Å) in the simulation are compatible with the EXAFS results (2.82 and 2.99 Å). The third neighbor cannot be detected by EXAFS because of the increasing Debye-Waller factor. This effect is clearly due to the covalent interactions between the chains. This is confirmed by performing computer simulations of an isolated infinite chain (i.e., with periodic boundary conditions along the chain axis only), which lead to structures with equal spacings between the atoms.

ELECTRONIC STRUCTURE

The change of the electronic structure upon melting is correlated with the change of the atomic structure. Figure 6 compares the average electronic densities of states calculated with a resolution better than 1 eV (20 moments) of a system of 1152 atoms in the solid (190 °C) and liquid (425 °C) states. The s band lies between -11 and -4 eV and has a negligible overlap with the p band. In the solid state, in agreement with the band structure calculations of Joannopoulos *et al.*³³ the p band presents a three-peak structure corresponding to the σ , lone pair (LP), and σ^* subbands. Upon melting, the most important change concerns the LP band, which is broadened in two large peaks separated by about 3.5 eV. This broadening of the LP band is due to the presence of a third neighbor. A resonance effect arises between two neighboring LP orbitals as one of the interchain distances is shortened. At the resolution of our calculations, the gap at the Fermi level, present in the solid, appears to be nearly filled in the liquid—a small dip still remains—thus explaining the semiconductor-to-(semi)metal transition that is observed experimentally.

DISCUSSION

Our results show that the key for understanding the structure of liquid tellurium is to be found in the interchain interactions that are, at least partly, of covalent nature. The increase of the coordination number with increasing temperature results from the breaking of the symmetry of the

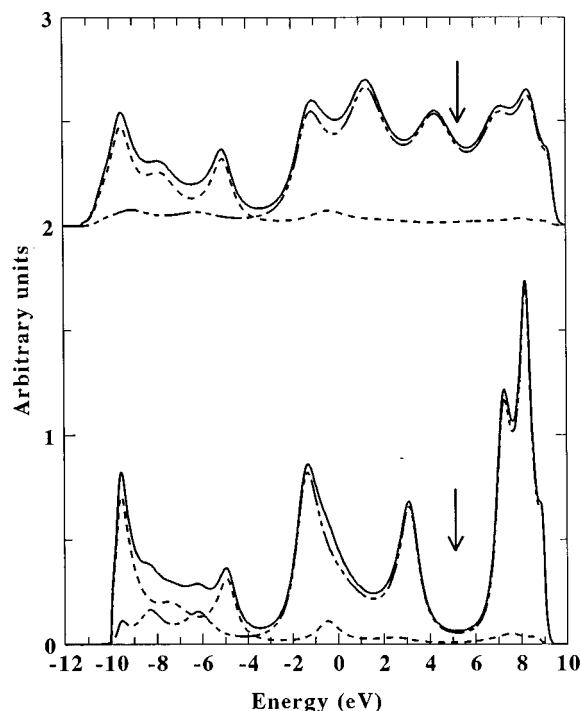


FIG. 6. Electronic density of states calculated with 20 exact moments (1152 atoms): lower part, solid at 190 °C; upper part, liquid at 480 °C. Dashed line, *s* electrons; dash-dotted line, *p* electrons; solid line, total density of states. The arrows indicate the Fermi level.

interchain neighbor shell upon melting. The local environment of each atom changes from two short and four long neighbor distances to two short, one medium, and three long neighbor distances. In agreement with the most recent EXAFS measurements,¹⁸ our calculations show a short-long alternation of the distances along the chains. The third distance (first interchain) contribution is too widely spread to be extracted from an EXAFS spectrum. Nevertheless, this shortened interchain bond is responsible for the broadening of the lone pair band of the electronic density of states of the solid, leading to a metallic conductivity. The resulting average local atomic structure is an asymmetric variant of the one proposed by Cabane and Friedel¹³ with a threefold coordination with three different neighbor distances. The symmetry-breaking process upon melting is governed by the gain in configurational entropy (there are four energetically equivalent ways of shortening one of the long bonds) and in electronic entropy (delocalization of the electrons of the lone pair band). Indeed, the experimental melting entropy is unusually high (24.16 J mol⁻¹ K⁻¹). Another possible origin could be an energy gain if the LP band is asymmetrically broadened.

Our results are not conclusive in this regard and a more detailed analysis of the electronic structure is required.

CONCLUSION

The computer simulations presented here not only help to understand the atomic and electronic structure of liquid tellurium, but are also able to reproduce quantitatively the structural data. The calculations are based on a simplified tight-binding model of the electronic interactions for the attractive part combined with an empirical pairwise repulsive potential. Other missing contributions to the total energy of the system, such as the dispersion term, are accounted for by an external pressure. The approximate description of the electronic density of states at the fourth-moment level proves accurate enough, as far as total energies are concerned, to successfully compare to the available experimental data on the atomic structure, among which are the most recent neutron scattering and EXAFS measurements. Large systems, up to 1152 atoms, corresponding to a cubic box with about a 35 Å edge, can be handled, thus reducing the artifacts inherent to small systems. The key role of the interchain covalent interactions is emphasized. In the crystalline state, as a result of the Peierls distortion, each atom builds up two strong and short (2.86 Å) covalent bonds with its neighbors in the chain and four longer (3.45 Å) and weaker bonds with the atoms belonging to neighboring chains. Upon melting, the local atomic environment is modified. The main effect is a significant reduction of one of the long bonds (around 3.10–3.20 Å, with a broad dispersion). On the one hand, the broad dispersion of the third-neighbor interchain bond length allows one to distinguish between twofold- and threefold-coordinated atoms: the atomic structure can then be viewed as “entangled broken chains”¹⁴ with an average chain length of around five bonds at the melting point. On the other hand, as the chain structure of the crystal remains essentially unaltered except for the short-long alternation of the bonds along the chain, these results support the conclusions drawn by other authors.^{8,17,18} The real situation lies in between the different points of view recalled in the Introduction, and the calculations that are presented here give clear insight into the atomic and electronic structure of liquid tellurium. In particular, the metallic conductivity of the liquid appears as a consequence of the resonance of the lone pair orbitals of two atoms belonging to neighboring chains.

ACKNOWLEDGMENT

A grant of computing time on the CRAY-YMP computer of the Institut Méditerranéen de Technologie is gratefully acknowledged.

¹J. C. Perron, Phys. Lett. **32A**, 169 (1970).

²G. Tourand and M. Breuil, C. R. Acad. Sci. B **270**, 109 (1970).

³Y. Waseda and S. Tamaki, Z. Naturforsch. **30**, 1655 (1975).

⁴I. Hawker, R. A. Howe, and J. E. Enderby, in *Proceedings of the Fifth International Conference on Amorphous and Liquid Semiconductors*, edited by J. Stuke and W. Brenig, 1974 (Taylor and Francis, London, 1974).

⁵S. Takeda, S. Tamaki, and Y. Waseda, J. Phys. Soc. Jpn. **55**, 11 (1984).

⁶M. E. Welland, M. Gay, and J. E. Enderby, in *The Physics of Disordered Systems*, edited by D. Adler *et al.* (Plenum, New York, 1985).

⁷A. Menelle, R. Bellissent, and A. M. Flank, Europhys. Lett. **4**, 705 (1987).

- ⁸A. Menelle, R. Bellissent, and A. M. Flank, *Physica B* **156&157**, 174 (1989).
- ⁹M. Misawa, *J. Phys. Condens. Matter* **4**, 9491 (1992).
- ¹⁰W. Hoyer, H. Neumann, and M. Wobst, *Z. Naturforsch.* **47**, 833 (1992).
- ¹¹H. Endo, T. Tsuzuki, M. Yao, Y. Kawakita, K. Shibata, T. Kamiyama, M. Misawa, and K. Suzuki, *J. Phys. Soc. Jpn.* **63**, 3200 (1994).
- ¹²T. Tsuzuki, A. Sano, Y. Kawakita, Y. Ohmasa, M. Yao, H. Endo, M. Inui, and M. Misawa, *J. Non-Cryst. Solids* **156-158**, 695 (1993).
- ¹³B. Cabane and J. Friedel, *J. Phys.* **32**, 73 (1971).
- ¹⁴J. Hafner, *J. Phys. Condens. Matter* **2**, 1271 (1990).
- ¹⁵M. Cutler, *Liquid Semiconductors* (Academic, New York, 1977).
- ¹⁶J. E. Enderby and A. C. Barnes, *Rep. Prog. Phys.* **53**, 85 (1990).
- ¹⁷H. Endo, *J. Non-Cryst. Solids*, **156-158**, 667 (1993).
- ¹⁸T. Tsuzuki, M. Yao, and H. Endo, *J. Phys. Soc. Jpn.* **64**, 485 (1995).
- ¹⁹Y. Tsuchiya and E. F. W. Seymour, *J. Phys. Condens. Matter* **18**, 4721 (1985).
- ²⁰D. Hohl and R. O. Jones, *Phys. Rev. B* **42**, 3856 (1991).
- ²¹G. Kresse, J. Furthmüller, and J. Hafner, *Phys. Rev. B* **50**, 13 181 (1994); F. Kirchhoff, N. Binggeli, G. Galli, and S. Massidda, *ibid.* **50**, 9063 (1994).
- ²²C. Bichara, A. Pellegatti, and J.-P. Gaspard, *Phys. Rev. B* **47**, 5002 (1993).
- ²³C. Bichara, A. Pellegatti, and J.-P. Gaspard, *Phys. Rev. B* **49**, 6581 (1994).
- ²⁴J.-P. Gaspard, F. Marinelli, and A. Pellegatti, *Europhys. Lett.* **3**, 1095 (1987).
- ²⁵L. Goodwin, A. J. Skinner, and D. G. Pettifor, *Europhys. Lett.* **9**, 701 (1989).
- ²⁶J. A. Majewski and P. Vogl, in *Cohesion and Structure*, edited by F. R. De Boer and D. G. Pettifor (North-Holland, Amsterdam, 1989), p. 287.
- ²⁷W. A. Harrison, *Electronic Structure and the Properties of Solids* (Freeman, San Francisco, 1980).
- ²⁸K. Aoki, O. Shimomura, and S. Minomura, *J. Phys. Soc. Jpn.* **48**, 551 (1980).
- ²⁹D. A. Young, *Phase Diagram of the Elements* (University of California Press, Berkeley, 1991).
- ³⁰M. P. Allen and D. J. Tildesley, *Computer Simulation of Liquids* (Clarendon, Oxford, 1989).
- ³¹H. Thurn and J. Ruska, *J. Non-Cryst. Solids* **22**, 331 (1976).
- ³²C. Wagner and H. Ruppertsberg, *At. Energy Rev.* **1**, 101 (1981).
- ³³J. D. Joannopoulos, M. Schlüter, and M. L. Cohen, *Phys. Rev. B* **11**, 2186 (1975).